Nonlinear Gulf Stream interaction with the deep western boundary current system: observations and a numerical simulation

By David E. Dietrich, Avichal Mehra †, Robert L. Haney ‡, Malcolm J. Bowman ¶ AND Yu-Heng Tseng

1. Motivation and objectives

Gulf Stream (GS) separation near its observed Cape Hatteras (CH) separation location, and its ensuing path and dynamics, is a challenging ocean modeling problem. If a model GS separates much farther north than CH, then northward GS meanders, which pinch off warm core eddies (rings), are not possible or are strongly constrained by the Grand Banks shelfbreak. Cold core rings pinch off the southward GS meanders. The rings are often re-absorbed by the GS. The important warm core rings enhance heat exchange and, especially, affect the northern GS branch after GS bifurcation near the New England Seamount Chain. This northern branch gains heat by contact with the southern branch water upstream of bifurcation, and warms the Arctic Ocean and northern seas, thus playing a major role in ice dynamics, thermohaline circulation and possible global climate warming. These rings transport heat northward between the separated GS and shelf slope/Deep Western Boundary Current system (DWBC). This region has nearly level time mean isopycnals. The eddy heat transport convergence/divergence enhances the shelfbreak and GS front intensities and thus also increases watermass transformation. The fronts are maintained by warm advection by the Florida Current and cool advection by the DWBC. Thus, the GS interaction with the DWBC through the intermediate eddy field is climatologically important.

Besides GS separation and mean path, realistic simulation of GS natural variability is important. GS separation occurs (by definition) when the shelfbreak current from the Florida Straits angles toward deeper water. If it does not separate at CH, the observed separation location, but separates much later as is common in North Atlantic Ocean models, it then remains too close to the shelfbreak to allow northward (shoreward) meanders to develop freely and pinch off warm core eddies (rings). The distance from the mean GS current to shelfbreak must be at least comparable to the Rossby radius of deformation for this to happen. The highly energetic, nonlinear turbulent GS system provides a significant amount of geophysical "noise" to the climate system. Such "noise" may affect climate through fundamentally nonlinear stochastic resonance (Velez-Belchi et al. 2001); such resonance may be associated with nonlinear effects of changes relating to freshwater sources and sinks (Rossby and Nilsson 2003), changes of North Atlantic Deep Water formation (Rahmstorf and Alley 2002) and nonlinear GS interaction with the DWBC seen in results of the present study. Such variability may be natural in the ocean by itself. For example, even with annual cycle forcing, constructed using observed annual cycle

† Mississippi State University
‡ Naval Postgraduate School
¶ State University of New York at Stony Brook

surface wind, heat flux and freshwater source/sink conditions, there may be significant interannual variability, as seen in Mediterranean Sea modeling studies (Fernandez et al. 2003). Another example of particularly strong natural interannual variability is the Gulf of Mexico (Dietrich et al. 1997), which is dominated by the Loop Current and its irregular major eddy shedding, independent of annual cycle forcing, having a mean time-scale of about 270 days.

Two recent major North Atlantic Basin model comparison studies are: DYNAMO (1997) and DAMEE-NAB (2000). None of the DYNAMO models at 1/3° horizontal resolution was able to simulate the observed GS separation at CH. This failure using only moderate horizontal resolution was not unexpected, because of the importance of fine-scale vorticity dynamics and bathymetry near CH (Dengg et al. 1996). Coastal abutments such as CH often lead to boundary current separation; examples are ubiquitous in nature, a prime example being the Black Sea whose coastal circulation is dominated by recirculation eddies in the wakes of coastal abutments (Staneva et al. 2001). Besides isobath curvature near the CH abutment, the upstream convergence of isobaths also plays an important role in GS separation (Stern 1998).

In the DAMEE model intercomparison experiment using HR (Hellerman and Rosenstein 1983) climatological wind forcing, all but one of the models failed to simulate GS separation at CH. The exception was ROMS (Haidvogel et al. 2000), which got GS separation at the proper location without resolving the major CH coastal abutment. Hurlburt and Hogan (2000) report that when sufficient resolution is used to address nonlinear GS separation dynamics at CH using the NLOM model (Hurlburt and Thompson 1980), realistic GS separation and other inherently nonlinear features are well simulated using HR winds, *even though* the linear version of the same model shows unrealistic wind-stress-curl-induced GS separation for 11 different wind stress climatologies including HR winds (Townsend et al. 2000). The linear effects of wind stress curl do not explain the observed GS separation and path, but instead give two paths, both very different from the observed one. Thus, the ROMS low resolution GS separation at CH is surprising.

Herein, we adapt the DieCAST ocean model to the North Atlantic/Caribbean Sea/Gulf of Mexico system in order to explore GS separation and ensuing dynamics. Base case results are discussed, focusing on GS interaction with the DWBC during a 75-year simulation. In follow up to this base case, closely related sensitivity studies (Dietrich et al. 2003b) show significant effects of horizontal viscosity and diffusivity, especially relating to the thin, narrow DWBC and its effects on GS separation.

The DieCAST ocean model adaptation for the present North Atlantic study is described in Section 2. In Section 3, the modeled North Atlantic general circulation is compared with observations, focusing on the GS and DWBC. Results before and after the establishment of the DWBC show dramatic effects of the DWBC on the GS separation and path. Further discussion of the significance of the DWBC is given in Section 4. Conclusion and future work are given in Section 5.

2. Model and Experiment Design

We use the z-level DieCAST ocean model adapted to the North Atlantic Ocean/ Caribbean Sea/ Gulf of Mexico system. The duo grid model runs at about 200 model days per day of computer time on a PC using a single 2.0 gigahertz P4.

The model uses:

a) fourth-order accurate numerical approximations for all terms, except a conventional

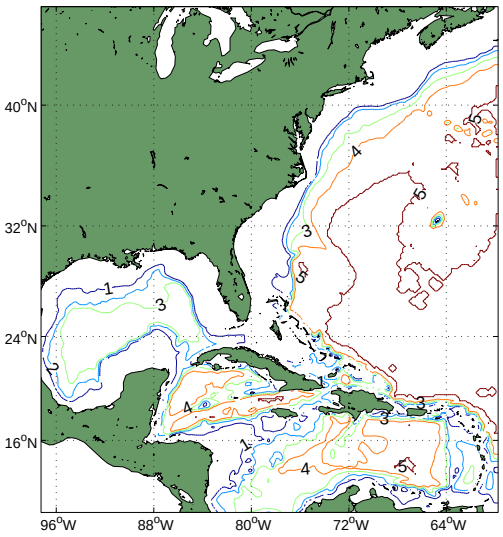

FIGURE 1. Western (1/6° resolution fine grid) domain bathymetry (depth is in km).

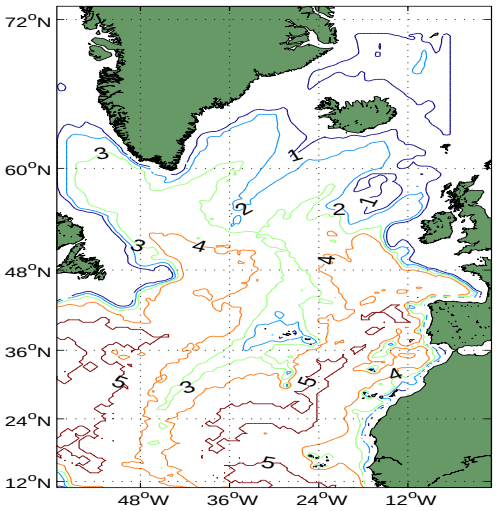

FIGURE 2. Eastern (1/2° deg resolution coarse grid) domain bathymetry (depth is in km) showing shelfbreak bathymetry in the shortcircuited Arctic Ocean.

second-order accurate hydrostatic vertical pressure gradient, in a semi-collocated control volume framework (Sanderson and Brassington 1998);

b) an incompressibility algorithm having low numerical dispersion associated with its required interpolations (Dietrich 1997)

The semi-collocated grid avoids the large numerical dispersion resulting from evaluating the large Coriolis term on the conventional staggered Arakawa "C" grid. Fourth-order accurate advection further reduces numerical dispersion. Thus, the model is formally accurate in all significant respects. It is also robust using very low total (explicit plus numerical) dissipation.

The model domain covers the North Atlantic basin from 10° N to 73° N and from 97.5° W to 0° W. To reduce the computation required, a duo grid approach is used; the grids are coupled using upwind-based boundary flux approximations as used by Dietrich and Mehra (1998) for the Santa Barbara Channel nested in the California Current system. The western North Atlantic, Gulf of Mexico and Caribbean Sea require high resolution to resolve the GS separation region and critical narrow straits. West of 60° W, 1/6° resolution is used; east of 60° W, 1/2° resolution is used. The grids are fully two-way coupled each time step, with one coarse grid cell overlap (3×3 fine grid cells). The results are virtually seamless at the duo grid interface (Dietrich 2002). There are 30 model layers, geometrically expanding from 41.6 m thick at the top to 738 m thick at the bottom (maximum depth 5000 m). Open southern boundary conditions are derived from a one degree global implementation of the DieCAST ocean model.

Figure 1 shows the western domain bathymetry. Figure 2 shows the eastern domain and has lower resolution than Figure 1. To avoid potentially disastrous unphysical vortex stretching in the northeast corner of the eastern domain, the real bathymetry is replaced by a shelfbreak patterned after the shortcircuited Arctic Ocean, rather than using a conventional vertical wall approach.

To resolve the critical Caribbean Sea passages and reduce computation, the duo grid

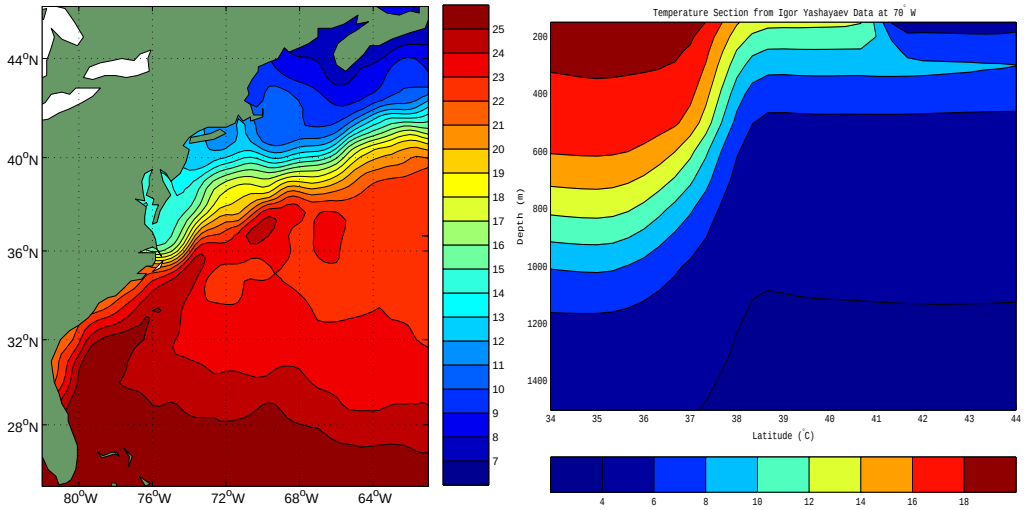

FIGURE 3. Surface layer annual mean Yashayaev temperature ($^\circ C$) climatology in the western domain GS region (west of 60 deg W) of the duo grid DieCAST north Atlantic model (left panel); Vertical/latitudinal cross-section of annual mean Yashayaev potential temperature ($^\circ C$) climatology at 70 deg W, showing highly nonlinear, non-diffusive flattening of isopycnals between Gulf Stream and Grand Banks (right panel).

interface is placed just east of the important Caribbean Sea passages, and the western fringe of the Labrador Sea (west of 60° W) is excluded and an idealized shelfbreak is used along 60° W in the eastern domain (Figure 2), again to minimize unrealistic vortex stretching. Surface boundary conditions are derived from monthly climatology. The wind forcing is by monthly average HR climatological winds. Levitus climatology is used for initial conditions and for surface thermohaline forcing until model year 13, when it is replaced by an improved (less smoothed) surface climatology (Yashayaev 2002). The annual mean surface temperature in the GS region from Yashayaev climatology (Figure 3) is consistent with the observed GS separation near CH.

Below-surface-layer model temperature is restored toward climatology in a buffer zone 20 gridpoints wide along open northern lateral boundaries. Salinity is not restored, because that does not conserve salt material and has no physical basis. Instead, a 0.2 Sv (1 Sverdrup equals one million cubic meters per second) inflow of freshwater is spread uniformly along the open northern boundary to parameterize Arctic Ocean net river inflow (Bacon et al. 2002) and a 0.018 Sv Gulf of St. Lawrence freshwater volume source is also specified (Chapman and Beardsley 1989). Heat and freshwater fluxes at the sea surface are computed such that the model multi-year mean annual cycle of surface temperature and salinity follow the observed climatological annual cycle (Dietrich et al. 2003a). This new surface buoyancy flux condition avoids problems (reduced annual cycle amplitudes and phase lags, and excessive damping of surface fronts) attributed to conventional restoring (Killworth et al. 2000).

All *externally* specified inflows are in the eastern, coarse grid domain; these are added to the western boundary inflow from the fine grid western domain and to the integrated evaporation-precipitation (e-p) to get a net eastern domain inflow (derived as described by Dietrich et al. 2003a); then, the total inflow is subtracted uniformly at the southern boundary (about 0.02 Sv as it turns out) to be consistent with incompressibility. An

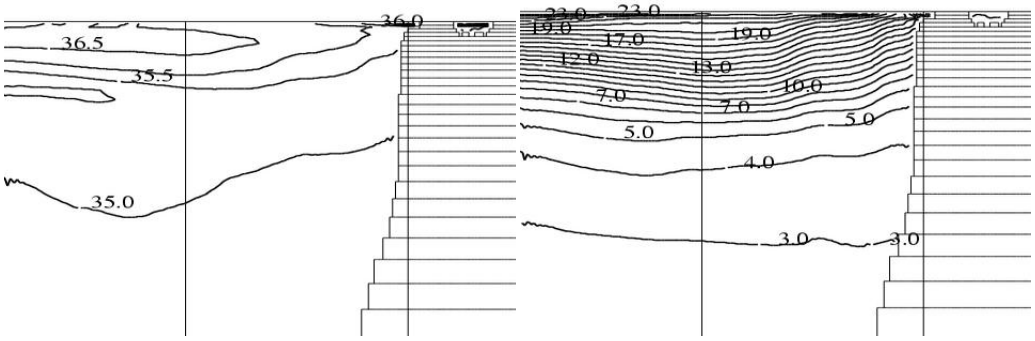

FIGURE 4. Vertical/latitudinal cross-sections at 70 deg W of time-averaged salinity (left) and temperature (right) during years 0-5.

alternate approach, not used here, is to apply this volume correction at the surface (e.g., in a global model having closed lateral boundaries), using the mean diffusivity between the top two layers to maintain observed climatological annual cycle surface layer salinity. This approach is consistent with the long-term climatological state (near zero mean sea level change) and with the rigid-lid approximation used in this model, in which there can be no mean surface height change. Thus, the rigid lid is slightly porous; the divergence of the barotropic mode (vertically integrated horizontal velocity) is very small but not exactly zero.

In the western (1/6° resolution) domain, we use constant horizontal viscosity and diffusivity of 10 m^2/sec. Based on the scale of the CH abutment curvature ($\sim$ 100 km) and GS velocity ($\sim$ 1 m/sec), this gives Reynolds number $O(10,000)$ for the primary GS separation scale. The Rossby number for these scales is $O(0.1)$. Both domains use near-molecular background vertical viscosity and diffusivity, with modified Pacanowski and Philander Richardson number based mixing as described by Staneva et al. (2001). Thus, the inertia terms are strong in the CH region, as necessary (but not sufficient, as a robust DWBC is also required, as will be shown here) for nonlinear inertial separation.

3. Results

3.1. *Before and After DWBC Interaction with GS Separation*

The transient GS behavior during the first five model years is strikingly different from the long-term behavior (Figures 4 - 6). During the first model year (not shown), bathymetry-induced strong inertial dynamics lead to early partial GS separation near CH. However, the separated portion of the model GS moves northward to the Grand Banks shelfbreak during the next few model years. It then moves back southward to its observed CH separation point and mean downstream path after about 10 model years, and remains close to the mean observed path throughout years $10-75$ (end of the present simulation).

It follows that model intercomparisons of the GS region before 10 years of simulation, such as done under DAMEE, are of limited value, especially when overly diffused, highly unstable (baroclinically) Levitus climatology is a basis for model comparison, even for time averaged model results, as will be seen below.

Figures 4 and 5 shows vertical/latitudinal cross-sections at 70° W of temperature averaged during years $1-5$ and years $66-75$ respectively. There is clearly a strong flattening of isopycnal surfaces (well approximated by isotherms) between the DWBC and

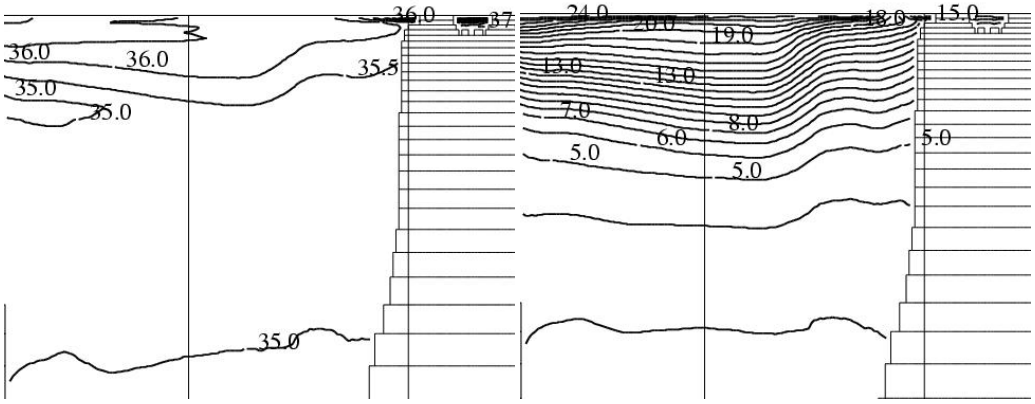

FIGURE 5. Vertical/latitudinal cross-sections at 70 deg W of time-averaged salinity (left) and temperature (right) during years 66-75.

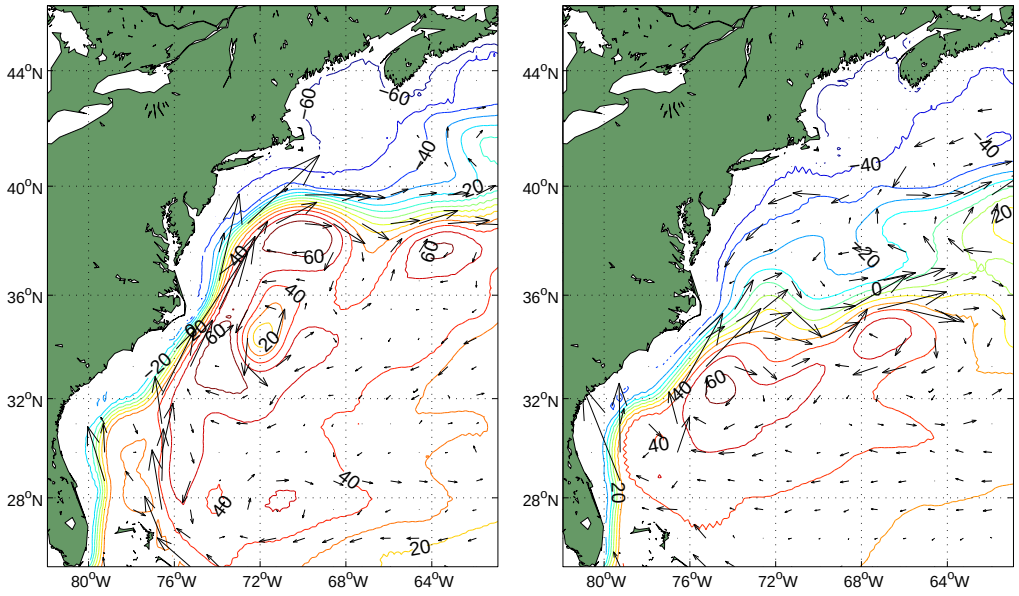

FIGURE 6. Time mean seasurface height (cm) and 700 m depth velocity vectors in the 1/6° resolution western domain during years $0-5$ (left) and during years $66-75$ (right).

GS core during the latter years (Figure 5), as in observations (Figure 3). Also during the latter years, there is a strong deepwater GS jet and front outcropping, as in observations.

Figure 6 shows the time mean surface pressure with superposed 700 m depth time-averaged velocity vectors during years $1-5$ and years $66-75$. The color shaded contour field is the time mean surface height. The arrows are time mean velocity vectors at 700m depth. The mean Gulf Stream front is the boundary between the green and light blue. The slight northward bend into the mid Atlantic Bight (a.k.a. "New York Bight") reflects warm core eddies that separate from northern tips of Gulf Stream meanders (mostly far downstream from Cape Hatteras), some of which slowly propagate all the way back to the Cape Hatteras region where they rejoin the Gulf Stream. Nearly all of the "blue water" in the mid Atlantic Bight (a.k.a. "New York Bight") is cold water that has upwelled

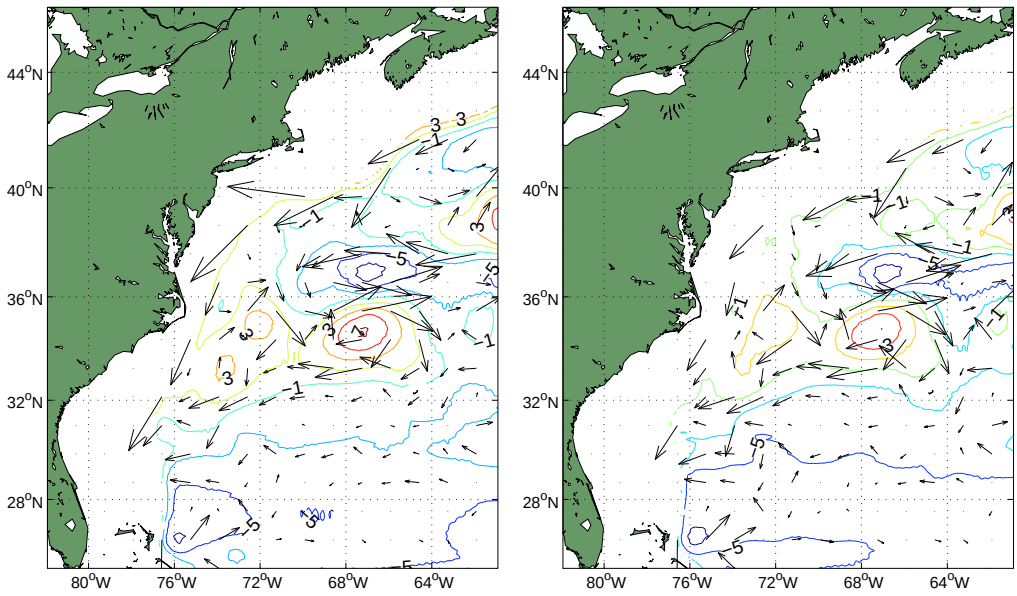

FIGURE 7. Time mean pressure and velocity vectors in the 1/6° resolution western domain during years $66-75$ at levels 1474 m (left) and 2020 m (right).

along the shelfbreak between south Florida and the mid Atlantic Bight region; this water recirculates back to the northern seas and Arctic Ocean after heat exchange with the warmer green water that recirculates southward along with the other "warmer colors" that indicate higher surface elevations. Apparently, the DWBC, indicated by the deep velocity vectors during years $66-75$, but missing during years $1-5$, plays a big role in the observed mean GS path.

The DWBC extends to more than 2000 m depth in the model results (Figure 7). After turning sharply counterclockwise near CH most of the DWBC current travels eastward to well off-shore, before turning southward, crossing under the GS and turning back towards the coast. Transient eddies are significant throughout the depth, and dominate in the deeper levels where the mean flow is smaller.

These figures show the dramatic effect of the DWBC on the GS and the major flattening of isopycnal surfaces that occurs after the DWBC dense water reaches the Grand Banks shelfbreak region. Dietrich et al. (2003b) find that a realistically narrower western Labrador Sea shelfbreak significantly intensifies the DWBC, resulting in even more strongly flattened isopycnals than seen in Figure 5, more like Yashayaev climatology (Figure 3). Higher model resolution may further intensify the DWBC, but is not addressed.

The negative contours in Figure 6 intersect the U.S. mainland coast *nearly* tangentially; this reflects upwelled DWBC water on the west side of the Florida Strait, as consistent with the cool coastal climatological temperature (Figure 3) and model temperature that is close to the climatology. This upwelling reflects a secondary circulation effect associated with bottom friction and mixing of offshore GS jet momentum into the slower moving coastal water. The strong GS jet effects dominate over local wind forcing, unlike the California Current system (Haney et al. 2001).

Thus, even the nearshore part of the coastal current, which is shoreward of the upwelled coastal water indicated by the negative contours in Figure 6, separates almost completely

at CH and forms the north wall of the separated GS. As noted above, this does not occur as a linear response to the HR winds used in this study.

The explanation of the interesting strong GS/DWBC interaction indicated by Figures 4-6 is as follows. The Levitus climatology used to initialize the model is unrealistically baroclinic between the observed GS mean location and the Grand Banks shelfbreak, reflecting diffusive smoothing of climatological data. The resulting baroclinic eddies transport potential density southward (mainly by northward heat transport) and flatten potential density contours in the deep offshore water, leading to strong isopycnal slopes in the shelfbreak region and much weaker slopes along the observed mean GS axis. Thus, there is a northward displacement of the GS front to the Grand Banks shelfbreak during the first few model years and a corresponding wrong GS path. Only after full establishment of the DWBC along the Grand Banks shelfbreak, which takes about 10 model years to occur, does the front move southward to its observed location. This is the time scale required for densest DWBC water formed in the GIN Sea to reach the Grand Banks.

Thus, overly diffusive models, carefully tuned to the diffuse Levitus climatology, can closely match this climatology. However, *it is impossible to tune models requiring such large diffusion to the observed flattened time averaged non-diffused climatological isopycnals* (Figure 3). This can only be done by a model such as the present DieCAST model configured with low diffusion (Figure 5).

Thus, the DWBC water plays a major material role in model GS separation. In a limited-area model having specified DWBC inflow, Thompson and Schmitz (1989) came to a similar conclusion. The role is analogous to the inner wall of rotating annulus experiments, except the cold water source is by advection of the dense DWBC water rather than by conduction at the wall. The GS, in turn, plays a role analogous to the outer wall of the rotating annulus experiments. Amplitude vacillation in those experiments is accompanied by flattening of interior isotherms due to baroclinic instability (Pfeffer et al. 1974), which by its very nature results in such flattening. This also characterizes the atmospheric index cycle.

3.2. *Other Significant Results*

A large northern recirculation gyre occurs between the GS and the Grand Banks shelfbreak at depth > 700 m. This gyre entrains and recirculates some of the DWBC water. Figure 8a shows its far north source, the East Greenland Current, flowing over the Denmark Strait, which preconditions even deeper water formation in the Labrador Sea. On the east side of the Denmark Strait, a fragment of the North Atlantic Gyre flows into the GIN Sea as observed. Notably, such two-way flow separated by a strong front occurs in spite of the coarse $1/2^\circ$ resolution used in the eastern domain of the present model. The sill overflow quickly becomes a quasi-balanced bottom density current, as the Coriolis terms quickly arrest any initial downslope flow (away from shore) to give a quasi-balanced along-isobath flow with deep water and lower pressure to the left (looking downstream); a slow, frictionally induced cross-isobath (away from shore) flow toward deeper water occurs in the bottom boundary layer.

Figure 9 shows the time mean rms velocity deviation from the time mean velocity at 700m depth in the Denmark Strait region, where dense sill level water spills "over the dam (sill)" into a bottom density current. This shows that the deep eddy activity is concentrated in the DWBC region (along the shelfbreak), where significant vortex stretching is driven by energy-releasing sinking dense DWBC water along the shelfbreak and by locally strong interaction with GS water near the northeast coast of the Flemish Cap (45 deg W, 47 deg N). The vortex stretching, as the potential energy is released,

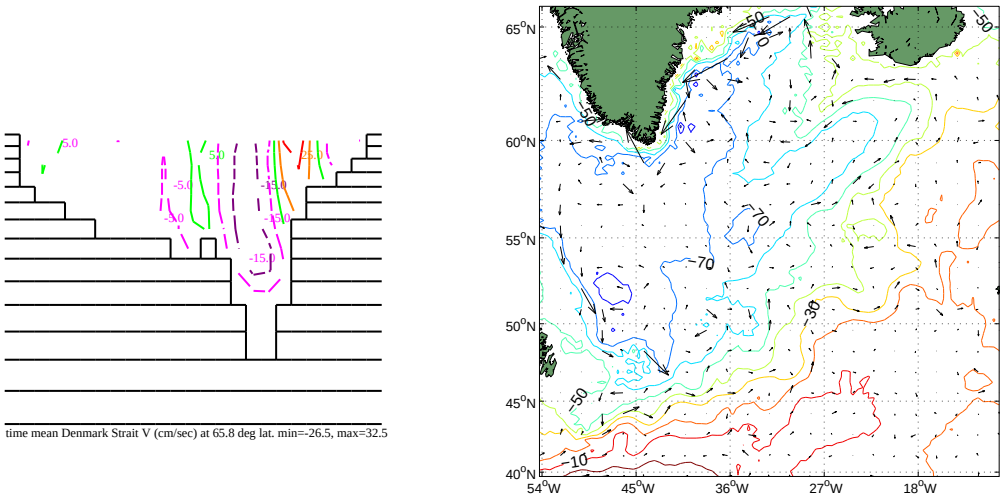

FIGURE 8. (a) Vertical/longitudinal cross-section of time mean latitudinal velocity across Denmark Strait in the coarse 1/2° resolution model eastern domain (left panel); (b) Time mean surface height and velocity vectors at 700 m depth in the Denmark Strait region (right panel).

results in turbulent mixing of the East Greenland Current (Arctic Ocean source) water with the North Atlantic Gyre water. The saddle point structure of the time average surface height (Figure 8b) reflects the sill bathymetry, and also shows the mean watermass paths leading to turbulent interaction. Thus, Figures 8-9 indicate inertial, turbulent interaction between the East Greenland Current and North Atlantic Gyre south of the Denmark Strait, even with the relatively coarse 1/2° resolution in this region. The sill overflow is an important part of the thermohaline circulation, and the associated locally strong mixing is important to watermass dynamics.

While some of the DWBC upwells on the north side of the GS separation point, some of it continues southward. Some of the southward branch upwells on along the shelfbreak between CH and the Bahamas. The cool coastal temperatures in both the Yashayaev climatology and the model results in this region reflect this upwelling. Horizontal advection by the Florida Current from the south that warms the coastal region is balanced by vertical advection and mixing. Such vertical circulation is forced by a combination of bottom drag and entrainment of coastal water into the strong GS current. This indirect circulation intensifies the GS front, thereby affecting development of eddies through baroclinic instability, especially after GS separation. Thus, in this narrow coastal region, the upwelled undercurrent water is entrained into the Florida Current from the south; this is a region of significant watermass mixing. Unlike the wind forced coastal jet of the California Current system (Haney et al. 2001), local wind effects may be secondary in such an energetic current system.

These mean results, calculated on a modern PC, are more realistic than the recent state-of-the-art results by Chao et al. 1996 despite requiring less overall resolution. Using realistic HR winds which, unlike the winds they used, do not *force* separation at CH (Townsend et al. 2000), the mean path of the model GS is very close to the observed mean path, starting with a realistic trajectory from the observed separation point. Further downstream, the separated upwelled coastal water bifurcates from the GS core, similar to the two-branch separated Gulf Stream in the linear response to HR winds noted by

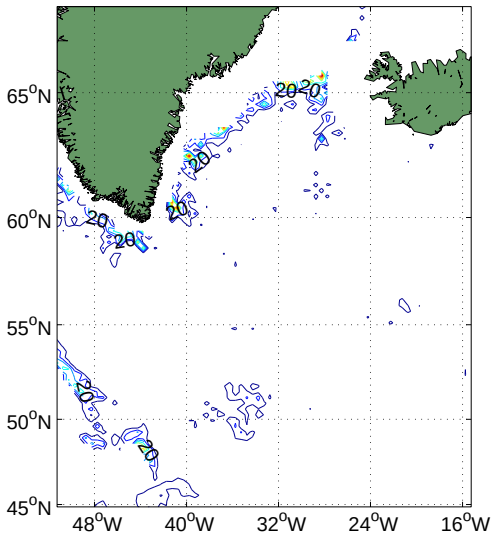

FIGURE 9. Time mean rms velocity deviation from the time mean velocity at 700 m depth in the Denmark Strait region.

Townsend et al. (2000), but is also influenced by interaction with the New England Seamount Chain, as indicated by the animation from Figure 10 (shown in `ftp://ssc.erc.msstate.edu/pub/mehra/nab_duo/OMO/year69-70.AVI.gz`).

Figure 10 shows a sequence of the surface currents during model year 70. A major cold core eddy (often called a ring) pinches off the southern tip of a southward GS meander around day 85. Around day 100, a warm core pinches off a northward meander. Later, another warm core develops as a result of GS interaction with the New England Seamount Chain. There is a deep northward secondary flow generated by blocking of the deep GS flow, which also steers the northern GS surface current fringe northward into a developing warm core ring, as discussed by Hurlburt and Thompson (1984). This GS bifurcation is a prevailing feature in model results, as indicated by Figure 6. The GS straightens out to its observed mean path after these two major eddy pinchoffs. These results are consistent with observations of transient small-scale features in and around the GS. The results of Chao et al. (1996) do not show such fine-scale features.

Several times per year, buoyant warm-core eddies pinch off northward meanders of the GS and drift westward and southwestward back through the Middle Atlantic Bight, as also seen in Figure 10. They become imbedded in the Middle Atlantic Bight shelfslope current and ultimately entrained back into the GS near CH (e.g. Bowman and Duedall 1975). However, the volume of slope water entrained, including its eddies, is only a fraction of the total $O(100$ Sv) GS transport. Full separation of the warm GS water occurs at CH, including a small volume of much cooler DWBC water upwelled along the shelfbreak between the Florida Strait and the Middle Atlantic Bight.

Also in the Figure 10 sequence, the Gulf of Mexico Loop Current penetrates northward and pinches off a major warm core eddy. The Dry Tortuga cyclone plays a significant role, as do other cyclonic frontal eddies that originate along the Yucatan shelfbreak, some of which merge into the Dry Tortuga eddy when the Loop Current is well extended into the Gulf of Mexico. Some frontal cyclones also pass through the Florida Strait. Before the major warm core eddy pinchoff, the Loop Current takes the shape of a square

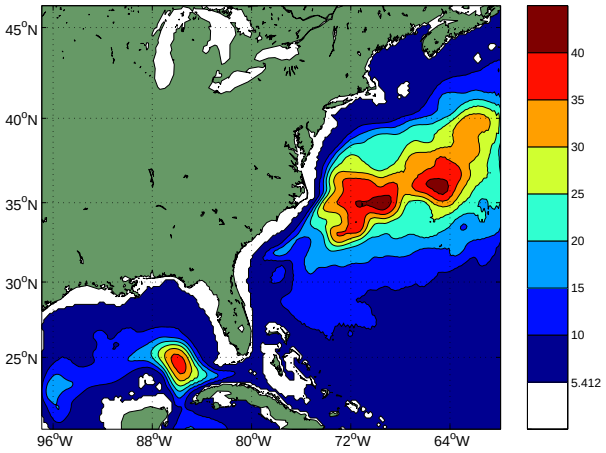

FIGURE 11. Root mean square deviation of surface height from years $66-75$ time mean in western $1/6^\circ$ resolution domain.

with rounded corners due to frontal eddy effects. The Loop Current takes a right angle turn into the Florida Strait after eddy shedding. Westward propagating anticyclones prevail in the Caribbean Sea, and there is a semi-permanent cyclonic recirculation in the southwestern Caribbean Sea corner. These details are consistent with observations and earlier modeling results (e.g. Dietrich et al. 1997).

Figure 11 shows rms seasurface height anomaly derived from the model results. In general, the rms value is $30-45$ cm along the separated GS axis all the way to the New England Seamount region near the eastern boundary of the $1/6^\circ$ resolution grid. Thus, vigorous transient eddies populate the modeled GS region with root-mean-square surface height anomaly amplitudes comparable to those in nature (DYNAMO 1997, Figure 8.6). The rms anomaly in the Gulf of Mexico region is also close to the observed, as in earlier Gulf of Mexico studies with DieCAST (Dietrich 1997; Dietrich et al. 1997). The rms value in the coarse resolution domain east of 60° W (not shown) is smaller, but there is a local maximum of about 20 cm along the shelfbreak at the south edge of the Flemish Cap. Coupling to low resolution coarse grid domain may cause reduced rms values near the eastern boundary in the fine grid domain.

4. DWBC Interaction with Methane Hydrates: Potential for Global Warming

Accurate DWBC simulation is important, because it not only affects the GS path as shown in Section 3, but the DWBC path also affects potential catastrophic release of vast amounts of methane gas from methane hydrates stored on the shelf slope below depths where methane freezes (about 4° C, depending also on pressure-depth). It is thought that this methane, after escaping to the atmosphere, may oxidize and add huge amounts of CO_2 (Katz et al. 1999), a greenhouse gas that, unlike the water vapor by-product, does not precipitate out, thus leading to global warming.

As suggested by Lai (2003), strongly exothermic biogeochemical processes occuring within the methane bubbles generated in the ocean depths (Kennett et al. 2000) may significantly warm the DWBC, lead to positive feedback, including by DWBC recirculation in the northern seas and Arctic ocean, and affect thermohaline circulation including Arctic and northern seas stratification through annual cycle ice melting/freezing. These

processes are coupled to the GS. The nonlinear GS/DWBC system dynamics may lead to accelerating methane release and sudden global warming. As further noted by Lai (2003), this possibility demands careful study, due to observed recent global warming (IPCC 2001) and oxygen depletion (Joos et al. 2003) in the ocean depths near the methane hydrate levels. A major concern is that anthropogenic perturbation of the system may lead to even stronger catastrophic warming than the about 10° C Arctic temperature rise that occurred in $10 - 20$ years at the end of the last glacial maximum (Rossby and Nilsson 2003).

The GS path affects the location and intensity of North Atlantic deep water formation, which occurs mainly in the northern seas and Arctic Ocean and feeds the DWBC after spilling over the GIN Sea sills. Its changes would alter the location and temperature of the DWBC, possibly augmenting the potential catastrophic greenhouse gas induced warming noted above. Modeling the DWBC water is a big challenge relating to GS separation. Dense fluid in a thin, narrow, bottom density current must travel from its high latitude source region to the Grand Banks shelfbreak without excessive numerical dissipation and dispersion, in order to have sufficient intensity to realistically affect the energetic GS separation and ensuing dynamics; this travel takes $O(10)$ years.

The dense narrow thin DWBC is not resolved by the climatological data used to initialize the model. Thus, it must develop spontaneously in the model. This dense shelfslope water forms in the northern seas, and takes more than a year to reach the Grand Banks from the Labrador Sea, and $O(10)$ years to reach there from the GIN Sea. In order for it to arrive at CH with sufficient intensity to properly affect GS separation and path, it must not be overly diluted by numerical dispersion and dissipation.

5. Conclusion and future work

Results presented herein show that one may simulate GS dynamics and separation from the coast realistically in a marginally eddy-resolving simulation by using a model having a) low total (physical plus numerical) dissipation; b) fourth-order accurate advection with its associated low numerical dispersion; c) further numerical dispersion reduction in the interpolations between grids; and d) fourth-order accurate horizontal pressure gradient. Nonlinear dynamics are involved in GS separation and it thus seems necessary to resolve the major CH abutment. However, although bathymetry-induced strongly inertial dynamics may favor separation near CH, our results indicate that is not sufficient; a robust DWBC is also required. A robust DWBC requires that the DWBC water not be dispersed by numerical errors during the $O(10)$ years to travel from its source region to the Grand Banks shelfbreak region. The importance of the DWBC is enhanced by its interaction with methane hydrates, which may lead to global warming.

It would be interesting to nest a finer grid in the GS separation region to shed more light on the detailed dynamics of the GS separation, focusing on the vertical circulation in the region of GS separation and how this circulation connects the GS to the DWBC. The significance of simulating a realistic GS/DWBC system lies partly in its potential impact on climate through fundamentally nonlinear stochastic resonance effects that are known to occur in many nonlinear systems (Rahmstorf and Alley 2002).

REFERENCES

Bacon, S., Reverdin, G., Rigor, I. G., & Smith, H. M. 2002 A freshwater jet on the East Greenland shelf. 2002 Ocean Sciences Meeting.

Bowman, M. J. & Duedall, I. W. 1975 Gulf Stream meander in the vicinity of the New York Bight. *Gulfstream*, **1** (2), 6–7, 1975. NOAA, Washington, D.C.

Chao, Y., Gangopadhyay, A., Bryan, F. O. & Holland, W. R. 1996 Modeling the Gulf Stream system: How far from reality?. *Geophys. Res. Lett.*, **23**, 3155–3158.

Chapman, D. C. & Beardsley, P. C. 1989 On the origin of shelf water in the Middle Atlantic Bight. *J. Phys. Oceanogr.*, **19**, 384–391.

DAMEE-NAB 2000 Data assimilation and model evaluation experiment - North Atlantic Basin. *Dyn. Atmos. Oceans.*, **32**, special DAMEE-NAB issue.

Dengg, J., Beckmann, A. & Gerdes R. 1996 The Gulf Stream separation problem. In: Krauss, W. (Ed.), The warmwatersphere of the North Atlantic Ocean. Gebr. Borntraeger, Berlin, 253–290.

Dietrich, D. E. 1997 Application of a modified "A" grid ocean model having reduced numerical dispersion to the Gulf of Mexico circulation. *Dynamics of Atmospheres and Oceans*, **27**, 201–217.

Dietrich, D. E. 2002 Duo-resolution North Atlantic Ocean/Gulf of Mexico model. 2002 Ocean Sciences Meeting.

Dietrich, D. E., Haney R. L., Fernandez V., Josey S. & Tintore, J. 2003a Air-sea fluxes based on observed annual cycle surface climatology and ocean model internal dynamics: a precise, non-damping, zero-phase-lag approach applied to the Mediterranean Sea. under revision.

Dietrich, D. E., Lin, C. A., Mestas-Nunez, A. & Ko, D.-S. 1997 A high resolution numerical study of Gulf of Mexico fronts and eddies. *Meteorol. Atmos. Phys.*, **64**, 187–201.

Dietrich, D. E. & Mehra, A. 1998 Sensitivity studies in the Santa Barbara Channel using the DieCAST ocean model. Proceedings of the Santa Barbara Channel Quality Review Board Meeting, San Diego, February, 1998.

Dietrich, D. E., Mehra, A., Richman, J., Bowman, M. J., Lai, C. A. & Tseng, Y. H. 2003b Nonlinear Gulf Stream interaction with the Deep Western Boundary Current System: bathymetry and dissipation sensitivity (to be submitted).

DYNAMO 1997 Dynamics of North Atlantic models. Simulation and assimilation with high resolution models. Institure fur Meereskunde an der Univsrsitat Kiel, 334.

Fernandez, V., Dietrich, D. E., Haney, R. L. & Tintore, J. 2003. Mesoscale, seasonal and interannual variability in the Mediterranean Sea using the DieCAST ocean model. Submitted to *J. Marine Systems* (in revision).

Haidvogel, D. B., Arango, H. G., Hedstrom, K., Beckmann, A., Malonotte-Rizzoli, P. & Shchepetkin, A. F. 2000 Model evaluation experiments in the North Atlantic Basin: simulations in nonlinear terrain-following coordinates. *Dyn. Atmos. Oceans.*, **32**, 239–281.

Haney, R. L., Hale, R. A. & Dietrich, D. E. 2001 Offshore propagation of eddy kinetic energy in the California Current. *JGR-Oceans*, **106**, 709–717.

Hellerman, S. & Rosenstein, M. 1983 Normal monthly wind stress over the world ocean with error estimates. *J. Phys. Oceanogr.*, **13**, 1093–1104.

Hurlburt, H. E. & Hogan, P. J. 2000 Impact of 1/8 deg to 1/64 deg resolution on Gulf Stream model-data comparisons in basin-scale subtropical Atlantic Ocean models. *Dyn. Atmos. Oceans.*, **32**, 283–329.

Hurlburt, H. E. & Thompson, J. D. 1980 A numerical study of Loop Current intrusions and eddy shedding. *J. Phys. Oceanogr.*, **10**, 1611–1651.

Hurlburt, H. E. & Thompson, J. D. 1984 Preliminary results from a numerical study of the New England Seamount chain influence on the Gulf Stream. Proc. of the Workshop on Predictability of Fluid Motions, Amer. Inst. Phys., G. Hollaway, Ed.

IPCC 2001 Climate change 2001: The scientific basis. Cambridge University Press, Cambridge, U.K. 881.

Joos, F., Platiner, G.-K., Stocker, T. F., Kortzinger, A. & Wallace, D. W. R., 2003 Trends in marine dissolved oxygen: Implications for ocean circulation changes and the carbon budget. EOS, *Transactions Ameri. Geophy. Union*, **84**, 197–201.

Katz, M. E., Pak, D. K., Dickens, G. R. & Miller, K. G. 1999 The source and fate of massive carbon input during the latest paleocene thermal maximum. *Science*, **286**, 1531–1533.

Kennett, J. P., Cannariato, K. G., Hendy, I. L. & Behl, R. J. 2000 Carbon isotopic evidence for methane hydrate instability during Quaternary Interstadials. *Science*, **288**, 128–133.

Killworth, P. D., Smeed, D. A. & Nurser, A. J. G. 2000 The effects on ocean models of relaxation toward observations at the surface. *J. Phys. Oceanogr.*, **30**, 160–174.

Lai, C.-C. A. 2003 personal communications.

Pfeffer, R. L., Buzyna, G. & Fowlis, W. W. 1974 Synoptic features and energetics of wave-amplitude vacillation in a rotating, differentially heated fluid. *J. Atmos. Sci.*, **31**, 622–645.

Rahmstorf, S. & Alley, R. B. 2002 Stochastic resonance in glacial climate. *EOS*, 19 March 2002 (lead article).

Rossby, T. & Nilsson, J. 2003 Current switching as the cause of rapid warming at the end of the last Glacial Maximum and Younger Dryas. *Geophys. Res. Lett.*, **30**. In press.

Sanderson, B.G. & Brassington, G. 1998 Accuracy in the context of a control-volume model. *Atmosphere-Ocean*, **36**, 355–384.

Staneva, J. V., Dietrich, D. E., Stanev, E. V. & Bowman, M. J. 2001 Rim current and coastal eddy mechanisms in an eddy-resolving Black Sea general circulation model. *J. Marine Systems*, special issue on the Black Sea, **31**, 137–157.

Stern, M. E. 1998 Separation of a density current from the bottom of a continental slope. *J. Phys. Oceanogr.*, **28**, 2040–2049.

Thompson, J. D. & Schmitz, W. J. 1989 A limited-area model of the Gulf Stream: design, initial experiments and model-data intercomparison. *J. Phys. Oceanogr.*, **19**, 791–814.

Townsend, T. L., Hurlburt, H. E. & Hogan, P. J. 2000 Modeled Sverdrup flow in the North Atlantic from 11 different wind stress climatologies. *Dyn. Atmos. Oceans.*, **32**, 373–417.

Velez-Belchi, P., Alvarez, A., Colet, P., Tintore, J. & Haney, R. L. 2001 Stochastic resonance in the thermohaline circulation. *Geophys. Res. Lett.*, **28**, 2053–2056.

Yashayaev, I. 2002 Personal communication.
http://www.mar.dfo-mpo.gc.ca/ science/ocean/woce/climatology/naclimatology.htm